Microwave Spectrum of Ethyl Cyanide; r_0-Structure, Nitrogen Quadrupole Coupling Constants and Rotation-Torsion-Vibration Interaction

H. Mäder, H. M. Heise, and H. Dreizler

Abt. Chemische Physik im Institut für Physikalische Chemie der Universität Kiel

(Z. Naturforsch. **29 a**, 164—183 [1973]; received October 27, 1973)

An investigation of the microwave spectra of ethyl cyanide CH_3CH_2CN and the isotopes CH_2DCH_2CN, CH_3CD_2CN was carried out. The ground vibrational state of CH_3CH_2CN was re-examined under high resolution to give three centrifugal distortion constants D_J, D_{JK} and D_K. From the rotational constants of the ground vibrational state of CH_3CH_2CN, CH_3CD_2CN, CH_2DCH_2CN (symmetric) and CH_2DCH_2CN (asymmetric), $CH_3CH_2{}^{13}CN$ and CD_3CHDCN a r_0-structure is derived. For the isotopes CH_3CD_2CN, CH_2DCH_2CN (symmetric) and CH_2DCH_2CN (asymmetric) the diagonal elements χ_{aa}, χ_{bb} and χ_{cc} of the quadrupole tensor with respect to the principal axes of inertia were deduced from the hyperfine structure of the rotational lines. The off-diagonal element χ_{ab} for CH_3CD_2CN and CH_2DCH_2CN (symmetric) and the principal elements χ_{zz}, χ_{xx} of the quadrupole coupling tensor were obtained from χ_{aa}, χ_{bb} of the two molecules and from the principal axis rotation angle about the c-axis produced by isotopic substitution. For the analysis of the rotational spectra in the first excited states of methyl torsion and the lowest frequency in plane bending vibration of normal ethyl cyanide a molecular model with two internal degrees of freedom is considered. From the rotational line splittings in both states the coefficients V_3 and V_6 of the Fourier expansion of the potential hindering the internal rotation of the methyl group are determined.

The microwave spectrum of ethyl cyanide (propionitrile) was previously studied by several authors. A molecular structure was proposed in an investigation by Lerner and Daily [1]. The emphasis of the microwave studies reported by Laurie [2] is on the dipole moment, ^{14}N-quadrupole coupling and barrier to internal rotation of the methyl group. The determination of the quadrupole coupling constants was completed by Li and Harmony [3].

Our microwave studies of ethyl cyanide were extended to further isotopic species of this molecule — CH_3CD_2CN and CH_2DCH_2CN — in order to obtain a more reliable r_0-structure as well as the principal elements of the quadrupole coupling tensor. A large part of this work is the investigation of the interaction of overall rotation and the two lowest frequency vibrations, which are the methyl-torsion and the CCN-in-plane bending vibration. The effects of this interaction have been observed in the rotational spectra of the first excited torsional and vibrational state of the normal molecule, CH_3CH_2CN.

Experimental

The microwave measurements were carried out in the frequency range from 8 to 41 GHz with a conventional 100 kHz Stark modulation microwave spectrograph [4, 5] employing phase stabilized BWO's as radiation sources. The absorption cell was cooled with methanol flowing through a cooling jacket. The measurements were performed at temperatures of approximately $-60\,^{\circ}$C and sample pressure of several microns.

Normal ethyl cyanide was obtained from Merck Company (Darmstadt) and was used without further purification. The isotopic ethyl cyanides, CH_3CD_2CN and CH_2DCH_2CN, were prepared from the corresponding deuterated ethyl iodides CH_3CD_2I (99 atom% D, Roth, Karlsruhe) and CH_2DCH_2I (98 atom% D, Sharp & Dohme, München). The method of preparation was a modified Kolbe reaction [6]. Sodium cyanide was dispersed in a solution of the ethyl iodide in triethyleneglycol at room temperature. The mixture was then heated slowly to 110 °C and held at this temperature for 1 hour. A magnetic stirrer war used to keep the sodium cyanide well dispersed throughout the mixture. The final product was isolated by distillation *in vacuo* and dried over P_2O_5. The purity of the sample was controlled gas chromatographically, the instrument used being a Beckman/GC-2 gas chromatograph (column, carbowax 400). Impurities found were the isonitrile and ethyl iodide. The sample purity of the ethyl cyanide was $\geqq 99.5\%$ so that additional purification was unnecessary.

Ground Vibrational State

All rotational transitions were clearly identified by their Stark pattern or nuclear quadrupole hyper-

Table 1. Rotational transitions [a] (MHz) for the ground vibrational state of normal ethyl cyanide CH_3CH_2CN.

Transition $J_{K_-K_+} - J'_{K_-'K_+'}$	$F - F'$	observed frequencies	unsplit frequencies	calculated frequencies [b]	$\Delta\nu$ HFS observed [c]	$\Delta\nu$ HFS calculated [d]	$\nu_{unspl} - \nu_{calc}$
$0_{00}-1_{01}$	1 — 2	8 949.40	8 949.26	8 949.28	0.14	0.17	— 0.02
	1 — 1	8 948.48			— 0.78	— 0.83	
	1 — 0	8 950.90			1.64	1.65	
$1_{01}-1_{10}$	2 — 2	23 427.89	23 428.14	23 428.15	— 0.25	— 0.27	— 0.01
	1 — 1	23 429.48			1.34	1.34	
	2 — 1	23 428.49			0.35	0.35	
	1 — 2	23 428.87			0.73	0.73	
	0 — 1	23 426.99			— 1.15	— 1.14	
$0_{00}-1_{11}$	1 — 2	31 898.23	31 898.29	31 898.41	— 0.06	— 0.06	— 0.12
	1 — 1	31 898.62			0.33	0.32	
	1 — 0	31 897.65			— 0.64	— 0.63	
$1_{01}-2_{02}$	2 — 3	17 891.07	17 891.00	17 891.06	0.07	0.07	— 0.06
	1 — 2	17 891.07			0.07	0.00	
	0 — 1	17 890.05			— 0.95	— 0.83	
	2 — 2	17 890.05			— 0.95	— 0.99	
	1 — 1	17 892.70			1.70	1.66	
$1_{10}-2_{11}$	2 — 3	18 377.91	18 377.71	18 377.67	0.20	0.19	0.04
	1 — 2	18 376.87			— 0.84	— 0.83	
	2 — 2	18 377.50			— 0.21	— 0.21	
	1 — 1	18 377.50			— 0.21	— 0.19	
$1_{11}-2_{12}$	2 — 3	17 419.77	17 419.56	17 419.63	0.21	0.21	— 0.07
	1 — 2	17 418.73			— 0.83	— 0.83	
	0 — 1	17 420.74			1.18	1.14	
	2 — 2	17 419.09			— 0.47	— 0.45	
$2_{02}-2_{11}$	3 — 3	23 914.69	23 914.84	23 914.76	— 0.15	— 0.15	0.08
	2 — 2	23 915.36			0.52	0.51	
	1 — 1	23 914.31			— 0.53	— 0.51	
	3 — 2	23 914.31			— 0.53	— 0.55	
	2 — 1	23 916.00			1.16	1.15	
	2 — 3	23 915.77			0.93	0.92	
	1 — 2	23 913.68			— 1.16	— 1.15	
$1_{01}-2_{12}$	2 — 3	40 368.58	40 368.59	40 368.76	— 0.01	— 0.02	— 0.17
	1 — 2	40 368.91			0.32	0.32	
	0 — 1	40 367.43			— 1.16	— 1.14	
	2 — 2	40 367.91			— 0.68	— 0.67	
	1 — 1	40 369.95			1.36	1.34	
$2_{20}-3_{21}$	3 — 4	26 878.48	26 878.23	26 878.20	0.25	0.24	0.03
	2 — 3	28 877.39			— 0.84	— 0.82	
	1 — 2	26 879.05			0.82	0.83	
$2_{02}-3_{03}$	3 — 4	26 817.85	26 817.80	26 817.86	0.05	0.04	— 0.06
	3 — 3	26 816.70			— 1.10	— 1.07	
	2 — 2	26 819.28			1.48	1.49	
$2_{11}-3_{12}$	3 — 4	27 561.70	27 561.61	27 561.64	0.09	0.08	— 0.03
	2 — 3	27 561.40			— 0.21	— 0.21	
	1 — 2	27 561.70			0.09	0.10	
$2_{12}-3_{13}$	3 — 4	26 124.76	26 124.68	26 124.65	0.08	0.09	0.03
	2 — 3	26 124.47			— 0.21	— 0.21	
	1 — 2	26 124.76			0.08	0.06	
	3 — 3	26 123.81			— 0.87	— 0.86	
	2 — 2	26 125.77			1.09	1.09	
$2_{21}-3_{22}$	3 — 4	26 848.93	26 848.69	26 848.53	0.24	0.24	0.16
	2 — 3	26 847.89			— 0.80	— 0.83	
	1 — 2	26 849.50			0.81	0.83	
$3_{03}-3_{12}$	4 — 4	24 658.58	24 658.73	24 658.54	— 0.15	— 0.10	0.19
	3 — 3	24 659.03			0.30	0.31	
	2 — 2	24 658.58			— 0.15	— 0.25	
	4 — 3	24 657.87			— 0.86	— 0.80	
	3 — 2	24 660.00			1.27	1.25	
	3 — 4	24 659.74			1.01	1.01	
	2 — 3	24 657.51			— 1.16	— 1.19	
$3_{30}-4_{31}$			35 814.10 [L]	35 814.41			— 0.31
$3_{31}-4_{32}$			35 814.10 [L]	35 813.98			0.12
$3_{21}-4_{22}$			35 866.1 [J]	35 866.02			0.08

Transition $J_{K_-K_+} - J'_{K_-'K_+'}$	$F - F'$	observed frequencies	unsplit frequencies	calculated frequencies[b]	$\Delta\nu$ HFS observed[c]	$\Delta\nu$ HFS calculated[d]	$\nu_{unspl} - \nu_{calc}$
$3_{22}-4_{23}$	4 — 5	35 792.24	35 792.07	35 791.91	0.17	0.12	0.16
	3 — 4	35 791.74			— 0.33	— 0.33	
	2 — 3	25 792.24			0.17	0.24	
$3_{12}-4_{13}$			36 739.67[L]	36 739.67			0.00
$3_{13}-4_{14}$			34 824.07	34 824.02			0.05
$3_{03}-4_{04}$			35 722.20	35 722.26			— 0.06
$4_{13}-3_{22}$	5 — 4	31 388.11	31 388.43	31 388.55	— 0.32	— 0.22	— 0.12
	4 — 3	31 389.04			0.61	0.61	
	3 — 2	31 388.11			— 0.32	— 0.43	
$4_{04}-4_{13}$	5 — 5	25 676.07	25 676.18	25 675.96	— 0.11	— 0.08	0.22
	4 — 4	25 676.41			0.23	0.23	
	3 — 3	25 676.07			— 0.11	— 0.16	
$5_{14}-4_{23}$	6 — 5	21 270.81	21 270.96	21 270.84	— 0.15	— 0.13	0.12
	5 — 4	21 271.28			0.32	0.32	
	4 — 3	21 270.81			— 0.15	— 0.20	
$4_{14}-5_{05}$			23 710.84	23 710.76			0.08
$5_{05}-5_{14}$	6 — 6	26 988.59	26 988.67	26 988.58	— 0.06	— 0.07	0.09
	5 — 5	26 988.85			0.18	0.19	
$5_{15}-6_{06}$			33 629.96	33 629.99			— 0.03
$6_{06}-6_{15}$	7 — 7	28 622.20	28 622.29	28 622.51	— 0.09	— 0.07	— 0.22
	6 — 6	28 622.47			0.18	0.17	

[a] All lines between 18 GHz and 41 GHz, except those labelled with L (taken from Ref. 2), were re-examined by H. Lutz. The transition $J = 1_{01} - 2_{12}$ had not been reported by earlier workers [1–3].
[b] Calculated with the rotational constants from Table 2 and Equation (1).
[c] Hyperfine component shifts $\Delta\nu$ HFS $= \nu_{observed} - \nu_{unsplit}$.
[d] Calculated with the quadrupole coupling constants from Reference 3.

fine structure. Due to the larger a-component of the electric dipole moment

$$(|\mu_a| = 3.78\,\text{D},\ |\mu_b| = 1.38\,\text{D},\ |\mu| = 4.02\,\text{D})^2$$

the μ_a-transitions are about 8 times more intense than the μ_b-lines of comparable line strength. We investigated only rotational transitions up to the rotational quantum number $J = 6$ for which no line splitting due to internal rotation of the methyl group was resolvable in the ground vibrational state.

The measured rotational transitions of the normal ethyl cyanide are listed in Table 1. The measured frequencies are compared with the spectrum of a centrifugal distorted asymmetric rotor. As the experimental data are not sufficient to determine all parameters in Watson's formula [7], we corrected the asymmetric rigid rotor energy levels $E_{JK_-K_+}(A, B, C)$ as follows:

$$E_{CD} = E_{JK_-K_+}(A, B, C) - D_J J^2 (J+1)^2 - D_{JK} J(J+1)\langle P_z^2\rangle - D_K \langle P_z^4\rangle \quad (1)$$

with A, B, C rotational constants $A \geqq B \geqq C$
D_J, D_{JK}, D_K centrifugal distortion constants
$\langle P_z^n\rangle$ expectation value of P_z^n ($n = 2, 4$) in the asymmetric rigid rotor eigenstate $E_{JK_-K_+}(A, B, C)$.

Equation (1) approximates Watson's formula for the near symmetric top. The molecular constants in (1), resulting from a least squares fitting procedure including all measured lines, are given in Table 2.

Table 2. Rotational constants (MHz) and moments of inertia [a] (amu Å^2) for the ground vibrational state of normal ethyl cyanide CH_3CH_2CN.

A	27 663.751 (± 0.074)[b]	I_a	18.268 52
B	4 714.157 (± 0.016)	I_b	107.203 89
C	4 235.135 (± 0.011)	I_c	119.329 37
D_J	0.0031 (± 0.0003)		
D_{JK}	— 0.041 (± 0.001)		
D_K	0.546 (± 0.019)		

[a] Conversion factor 5.05376×10^5 MHz amu Å^2.
[b] Standard errors obtained from the least squares fit including all unsplit line frequencies of Table 1.

The rotational line frequencies of 1,1-dideutero-ethyl cyanide, CH_3CD_2CN, are listed in Table 3. The measurements are compared with an asymmetric rigid rotor pattern obtained from a least squares fit including the rotational transitions up to $J = 2$. The rotational constants and moments of inertia are given in Table 4.

In the case of 2-monodeutero-ethyl cyanide, CH_2DCH_2CN, two rotational spectra were found corresponding to the position of the deuteron with

Table 3. Rotational transitions (MHz) for the ground vibrational state of CH_3CD_2CN.

Transition $J_{K_-K_+} - J'_{K_-'K_+'}$	$F - F'$	observed frequencies	unsplit frequencies	calculated frequencies[a]	$\Delta\nu$ HFS observed	$\Delta\nu$ HFS calculated[b]	$\nu_{unspl} - \nu_{calc}$
$0_{00}-1_{01}$	1 — 2	8 688.27	8 688.10	8 688.06	0.17	0.17	0.04
	1 — 1	8 687.24			— 0.86	— 0.86	
	1 — 0	8 689.81			1.71	1.72	
$1_{01}-1_{10}$	2 — 2	17 854.86	17 855.12	17 855.15	— 0.26	— 0.27	0.03
	1 — 1	17 856.51			1.39	1.37	
	2 — 1	17 855.47			0.35	0.34	
	1 — 0	17 854.86			— 0.26	— 0.16	
	1 — 2	17 855.90			0.78	0.76	
	0 — 1	17 853.92			— 1.20	— 1.21	
$0_{00}-1_{11}$	1 — 2	26 030.71	26 030.77	26 030.81	— 0.06	— 0.07	— 0.04
	1 — 1	26 031.12			0.35	0.35	
	1 — 0	26 030.07			— 0.70	— 0.70	
$1_{01}-2_{02}$	2 — 3	17 364.93	17 364.86	17 364.94	0.07	0.07	— 0.08
	1 — 2	17 364.93			0.07	0.00	
	0 — 1	17 363.88			— 0.98	— 0.86	
	2 — 2	17 363.88			— 0.98	— 1.04	
	1 — 1	17 366.57			1.71	1.73	
$1_{10}-2_{11}$	2 — 3	17 888.73	17 888.53	17 888.52	0.20	0.20	0.01
	1 — 2	17 887.67			— 0.86	— 0.86	
	0 — 1	17 889.90			1.37	1.37	
	2 — 2	17 888.35			— 0.18	— 0.25	
	1 — 1	17 888.35			— 0.18	— 0.16	
$1_{11}-2_{12}$	2 — 3	16 863.99	16 863.77	16 863.72	0.22	0.22	0.05
	1 — 2	16 862.89			— 0.88	— 0.86	
	0 — 1	16 864.99			1.22	1.21	
	2 — 2	16 863.33			— 0.44	— 0.44	
	1 — 1	16 863.99			0.22	0.16	
$2_{02}-2_{11}$	3 — 3	18 378.64	18 378.78	18 378.74	— 0.14	— 0.15	0.04
	2 — 2	18 379.30			0.52	0.51	
	1 — 1	18 378.25			— 0.53	— 0.51	
	3 — 2	18 378.25			— 0.53	— 0.60	
	2 — 1	18 380.00			1.22	1.21	
	2 — 3	18 379.78			1.00	0.96	
	1 — 2	18 377.55			— 1.23	— 1.21	
$1_{01}-2_{12}$	2 — 3	34 206.47	34 206.49	34 206.47	— 0.02	— 0.03	0.02
	1 — 2	34 206.84			0.35	0.35	
	0 — 1	34 205.28			— 1.21	— 1.21	
	2 — 2	34 205.80			— 0.69	— 0.68	
	1 — 1	34 207.87			1.38	1.37	
$2_{12}-3_{13}$	3 — 4	25 288.71	25 288.61	25 288.66	0.10	0.10	— 0.05
	2 — 3	25 288.41			— 0.20	— 0.22	
	1 — 2	25 288.71			0.10	0.07	
$2_{20}-3_{21}$	3 — 4	26 109.23	26 108.98	26 108.90	0.25	0.25	0.08
	2 — 3	26 108.10			— 0.88	— 0.86	
	1 — 2	26 109.86			0.88	0.86	
	3 — 3	26 109.23			0.25	0.25	
	2 — 2	26 108.10			— 0.88	— 0.87	
$2_{02}-3_{03}$	3 — 4	26 019.22	26 019.24	26 019.47	— 0.02	0.04	— 0.23
	2 — 3	26 019.22			— 0.02	0.00	
	1 — 2	26 019.22			— 0.02	— 0.17	
	3 — 3	26 018.12			— 1.12	— 1.11	
	2 — 2	26 020.77			1.53	1.56	
$2_{11}-3_{12}$	3 — 4	26 825.63	26 825.54	26 825.71	0.09	0.09	— 0.17
	2 — 3	26 825.34			— 0.20	— 0.22	
	1 — 2	26 825.63			0.09	0.10	
	3 — 3	26 824.90			— 0.64	— 0.67	
	2 — 2	26 826.32			0.78	0.80	
$3_{03}-3_{12}$	4 — 4	19 185.08	19 185.23	19 184.98	— 0.15	— 0.10	0.25
	3 — 3	19 185.54			0.31	0.30	
	2 — 2	19 185.08			— 0.15	— 0.24	

[a] Calculated with the rotational constants from Table 4 and asymmetric rigid rotor formula.
[b] Hyperfine component shifts calculated with the quadrupole coupling constants from Table 11.

respect to the symmetry plane of the molecule. The molecule may be called CH_2DCH_2CN (symmetric) or CH_2DCH_2CN (asymmetric) depending on whether the deuteron is positioned in or out of plane.

Table 4. Rotational constants (MHz) with standard errors [a] and moments of inertia (amu Å²) for the ground vibrational state of CH_3CD_2CN.

A	21 942.980 ($\pm$ 0.027)	I_a	23.031 32
B	4 600.231 ($\pm$ 0.015)	I_b	109.858 83
C	4 087.830 ($\pm$ 0.014)	I_c	123.629 40

[a] Obtained from least squares analysis including all unsplit line frequencies of Table 3 up to $J=2$.

The rotational frequencies and molecular constants of both isomeric forms are given in Tables 5, 6, 7 and 8. The rotational constants and the frequencies calculated from these constants are derived from a least squares analysis of rotational lines up to $J=2$, analogous to the case of the CH_3CD_2CN isotope.

Table 6. Rotational constants (MHz) with standard errors [a] and moments of inertia (amu Å²) for the ground vibrational state of CH_2DCH_2CN (sym.).

A	27 650.897 ($\pm$ 0.049)	I_a	18.277 02
B	4 425.142 ($\pm$ 0.027)	I_b	114.205 60
C	4 000.821 ($\pm$ 0.019)	I_c	126.318 07

[a] Obtained from least squares analysis including all unsplit line frequencies of Table 5 up to $J=2$.

Table 8. Rotational constants (MHz) with standard errors [a] and moments of inertia (amu Å²) for the ground vibrational state of CH_2DCH_2CN (asym.).

A	25 022.652 ($\pm$ 0.041)	I_a	20.196 74
B	4 583.476 ($\pm$ 0.022)	I_b	110.260 42
C	4 110.264 ($\pm$ 0.016)	I_c	122.954 63

[a] Obtained from a least squares analysis including all unsplit line frequencies of Table 7 up to $J=2$.

r_0-Structure

Lerner and Daily [1] derived six r_0-structure parameters from six rotational constants, which are the B and C constants of normal ethyl cyanide and of the $CH_3CH_2{}^{13}CN$ and CD_3CHDCN isotopes. This experimental information appeared to us be insufficient to obtain reliable values for the proposed structural parameters. Therefore, we decided to revise the r_0-structure taking into account all available experimental data. The structure fitting calculations were based on a least squares procedure including the rotational constants A, B, C of CH_3CH_2CN, CH_3CD_2CN, CH_2DCH_2CN (sym.), CH_2DCH_2CN (asym.), $CH_3CH_2{}^{13}CN$ and B, C of CD_3CHDCN. The error equations were weighted with the relative uncertainties of the rotational constants given in Table 10. The A rotational constant of $CH_3CH_2{}^{13}CN$ was calculated from the B and C constants and the inertia defect of normal ethyl cyanide with the assumption that the inertia defect is equal for both molecules.

Table 9. r_0-structural parameters of ethyl cyanide.

r_{C-C}	= 1.525 $\pm$ 0.003 [a] Å	
r_{C-CN}	= 1.427 $\pm$ 0.015 Å	
r_{C-N}	= 1.168 $\pm$ 0.021 Å	
r_{C-H} [b]	= 1.087$_1$ $\pm$ 0.0013 Å	(methylene)
r_{C-H} [b]	= 1.087$_3$ $\pm$ 0.0006 Å	(methyl)
$\sphericalangle$ CCN	= 180° (assumed)	
$\sphericalangle$ CCC	= 110.9 $\pm$ 0.1°	
$\sphericalangle$ CCH	= 111.2 $\pm$ 0.2°	(methyl)
$\sphericalangle$ HCH [d]	= 107.6°	(methyl)
$\sphericalangle$ CCH	= 111.8 $\pm$ 0.4°	(methylene)
$\sphericalangle$ HCCH [c]	= 59.8 $\pm$ 0.3°	(methylene)
$\sphericalangle$ HCH [d]	= 106.7°	(methylene)

[a] Standard errors obtained from the least squares procedure.
[b] $r_{C-H} = r_{C-D}$ assumed.
[c] Dihedral angle formed by in-plane methyl H, the two ethyl C and methylene H.
[d] Calculated from the other structure parameters.

Assuming that ethyl cyanide has C_s-configuration symmetry and deuteration does not change bond distances and bond angles, the number of independent structural parameters reduces to 13.

An attempt to fit all these parameters leads to ill-conditioned normal equations. To improve these equations we assumed further that the CCN-bond angle is equal to 180°, that the methyl group is C_3-symmetric, and that its symmetry axis is coaxial with the CC-bond axis (ethyl group). The least squares analysis then yields a r_0-structure which is given in Table 9 by 9 independent structural parameters. The larger standard errors of the CN- and CC-bond distances (cyano group) indicate high correlation between both parameters. In order to obtain more precise values and finally a r_s-structure we have begun the microwave investigation of further isotopic species of this molecule. The proposed structure for the ethyl cyanide molecule is illustrated in Figure 1. The rotational constants resulting from this structure are compared with the experimental values in Table 10.

Table 5. Rotational transitions (MHz) for the ground vibrational state of CH_2DCH_2CN (symmetric).

Transition $J_{K_-K_+} - J'_{K_-'K_+'}$	$F - F'$	observed frequencies	unsplit frequencies	calculated frequencies[a]	$\Delta\nu$ HFS observed	$\Delta\nu$ HFS calculated[b]	$\nu_{unspl} - \nu_{calc}$
$0_{00}-1_{01}$	1 — 2	8426.12	8425.95	8425.96	0.17	0.17	— 0.01
	1 — 1	8425.12			— 0.83	— 0.83	
	1 — 0	8427.60			1.65	1.66	
$1_{01}-1_{10}$	2 — 2	23649.77	23650.02	23650.08	— 0.25	— 0.27	— 0.06
	1 — 1	23651.35			1.33	1.33	
	2 — 1	23650.36			0.34	0.34	
	1 — 0	23649.77			— 0.25	— 0.17	
	1 — 2	23650.75			0.73	0.73	
	0 — 1	23648.86			— 1.16	— 1.16	
$0_{00}-1_{11}$	1 — 2	31651.58	31651.64	31651.72	— 0.06	— 0.07	— 0.08
	1 — 1	31651.96			0.32	0.33	
	1 — 0	31651.01			— 0.63	— 0.66	
$1_{01}-2_{02}$	2 — 3	16846.09	16846.04	16846.17	0.05	0.07	— 0.13
	1 — 2	16846.09			0.05	0.00	
	0 — 1	16845.10			— 0.94	— 0.83	
	2 — 2	16845.10			— 0.94	— 1.00	
	1 — 1	16847.72			1.68	1.66	
$1_{10}-2_{11}$	2 — 3	17276.47	17276.28	17276.25	0.19	0.19	0.03
	1 — 2	17275.44			— 0.84	— 0.83	
	0 — 1	17277.62			1.34	1.33	
	2 — 2	17276.10			— 0.18	— 0.23	
	1 — 1	17276.10			— 0.18	— 0.17	
$1_{11}-2_{12}$	2 — 3	16427.90	16427.71	16427.61	0.19	0.21	0.10
	1 — 2	16426.89			— 0.82	— 0.83	
	0 — 1	16428.87			1.16	1.16	
	2 — 2	16427.32			— 0.39	— 0.44	
	1 — 1	16427.90			0.19	0.17	
$2_{02}-2_{11}$	3 — 3	24080.10	24080.24	24080.16	— 0.14	— 0.14	0.08
	2 — 2	24080.76			0.52	0.50	
	1 — 1	24079.71			— 0.53	— 0.50	
	3 — 2	24079.71			— 0.53	— 0.57	
	2 — 1	24081.40			1.16	1.16	
	2 — 3	24081.19			0.95	0.93	
	1 — 2	24079.09			— 1.15	— 1.16	
$1_{01}-2_{12}$	2 — 3	39653.39	39653.41	39653.36	— 0.02	— 0.02	0.05
	1 — 2	39653.74			0.33	0.33	
	0 — 1	39652.25			— 1.16	— 1.16	
	2 — 2	39652.73			— 0.68	— 0.67	
	1 — 1	39654.72			1.31	1.33	
$2_{20}-3_{21}$	3 — 4	25301.85	25301.60	25300.93	0.25	0.24	0.67
	2 — 3	25300.75			— 0.85	— 0.83	
	1 — 2	25302.42			0.82	0.83	
	3 — 3	25301.85			0.25	0.24	
	2 — 2	25300.75			— 0.85	— 0.84	
$2_{02}-3_{03}$	3 — 4	25254.55	25254.56	25254.85	— 0.01	0.04	— 0.29
	2 — 3	25254.55			— 0.01	0.00	
	1 — 2	25254.55			— 0.01	— 0.16	
	3 — 3	25253.48			— 1.08	— 1.07	
	2 — 2	25256.04			1.48	1.50	
$2_{12}-3_{13}$	3 — 4	24638.11	24638.13	24637.83	— 0.02	0.09	0.30
	2 — 3	24638.11			— 0.02	— 0.21	
	1 — 2	24638.11			— 0.02	0.07	
	3 — 3	24637.23			— 0.90	— 0.85	
	2 — 2	24639.39			1.26	1.07	
$2_{21}-3_{22}$	3 — 4	25278.93	25278.71	25277.89	0.22	0.24	0.82
	2 — 3	25277.89			— 0.82	— 0.83	
	1 — 2	25279.53			0.82	0.83	
	3 — 3	25278.93			0.22	0.24	
	2 — 2	25277.89			— 0.82	— 0.83	

[a] Calculated with the rotational constants from Table 6 and asymmetric rigid rotor formula.
[b] Hyperfine component shifts calculated with the quadrupole coupling constants from Table 11.

Table 7. Rotational transitions (MHz) for the ground vibrational state of CH_2DCH_2CN (asymmetric).

Transition $J_{K_-K_+} - J'_{K_-'K_+'}$	$F - F'$	observed frequencies	unsplit frequencies	calculated frequencies[a]	$\Delta\nu$ HFS observed	$\Delta\nu$ HFS calculated[b]	$\nu_{unspl} - \nu_{calc}$
$0_{00}-1_{01}$	1 — 2	8693.90	8693.73	8693.74	0.17	0.16	— 0.01
	1 — 1	8692.91			— 0.82	— 0.82	
	1 — 0	8695.38			1.65	1.65	
$1_{01}-1_{10}$	2 — 2	20912.08	20912.34	20912.40	— 0.26	— 0.27	— 0.06
	1 — 0	20912.08			— 0.26	— 0.23	
	0 — 1	20911.25[c]			— 1.09	— 1.12	
$0_{00}-1_{11}$	1 — 2	29132.80	29132.85	29132.92	— 0.05	— 0.06	— 0.07
	1 — 1	29133.14			0.29	0.29	
	1 — 0	29132.24			— 0.61	— 0.59	
$1_{01}-2_{02}$	2 — 3	17379.30	17379.24	17379.36	0.06	0.07	— 0.12
	1 — 2	17379.30			0.06	0.00	
	0 — 1	17378.30			— 0.94	— 0.82	
	2 — 2	17378.30			— 0.94	— 0.99	
	1 — 1	17380.89			1.65	1.65	
$1_{10}-2_{11}$	2 — 3	17860.90	17860.71	17860.69	0.19	0.19	0.02
	1 — 2	17859.89			— 0.82	— 0.82	
	0 — 1	17862.05			1.34	1.35	
	2 — 2	17860.51			— 0.20	— 0.19	
	1 — 1	17860.51			— 0.20	— 0.23	
$1_{11}-2_{12}$	2 — 3	16914.57	16914.36	16914.27	0.21	0.21	0.09
	1 — 2	16913.55			— 0.81	— 0.82	
	0 — 1	16915.46			1.10	1.12	
	2 — 2	16913.89			— 0.47	— 0.47	
	1 — 1	16914.57			0.21	0.23	
$2_{02}-2_{11}$	3 — 3	21393.64	21393.79	21393.72	— 0.15	— 0.15	0.07
	2 — 2	21394.32			0.53	0.53	
	1 — 1	21393.27			— 0.52	— 0.53	
	3 — 2	21393.27			— 0.52	— 0.53	
	2 — 1	21394.91			1.12	1.12	
	2 — 3	21394.71			0.92	0.91	
	1 — 2	21392.69			— 1.10	— 1.12	
$1_{01}-2_{12}$	2 — 3	37353.47	37353.49	37353.44	— 0.02	— 0.01	0.05
	1 — 2	37353.78			0.29	0.29	
	0 — 1	37352.37			— 1.12	— 1.12	
	2 — 2	37352.79[c]			— 0.70	— 0.69	
$2_{20}-3_{21}$	3 — 4	26114.43	26114.20	26113.69	0.23	0.23	0.51
	2 — 3	26113.38			— 0.82	— 0.82	
	1 — 2	26115.00			0.80	0.82	
	3 — 3	26114.43			0.23	0.24	
	2 — 2	26113.38			— 0.82	— 0.83	
$2_{02}-3_{03}$	3 — 4	26048.42	26048.44	26048.75	— 0.02	0.04	— 0.31
	2 — 3	26048.42			— 0.02	0.00	
	1 — 2	26048.42			— 0.02	— 0.16	
	3 — 3	26047.37			— 1.07	— 1.06	
	2 — 2	26049.88			1.44	1.49	
$2_{11}-3_{12}$	3 — 4	26785.70	26785.62	26785.92	0.08	+ 0.08	— 0.30
$2_{12}-3_{13}$	3 — 4	25366.43	25366.35	25366.37	0.08	0.09	— 0.02
	2 — 3	25366.14			— 0.21	— 0.21	
	1 — 2	25366.43			0.08	0.06	
	3 — 3	25365.49			— 0.86	— 0.88	
	2 — 2	25367.42			1.07	1.12	
$2_{21}-3_{22}$	3 — 4	26082.13	26081.88	26081.22	0.25	0.24	0.66
	2 — 3	26081.06			— 0.82	— 0.82	
	1 — 2	26082.68			0.80	0.82	
	3 — 3	26082.13			0.25	0.24	
	2 — 2	26081.06			— 0.82	— 0.82	
$3_{03}-3_{12}$	4 — 4	22130.96	22131.11	22130.89	— 0.15	— 0.11	0.22
	3 — 3	22131.42			0.31	0.33	
	2 — 2	22130.96			— 0.15	— 0.26	
	4 — 3	22130.33			— 0.78	— 0.78	
	3 — 2	22132.07			0.96	1.23	
	3 — 4	22132.07			0.96	1.00	
	2 — 3	22129.94			— 1.17	— 1.16	

[a] Calculated with the rotational constants from Table 8 and asymmetric rigid rotor formula.
[b] Hyperfine component shifts calculated with the quadrupole coupling constants from Table 11.
[c] Further components obscured by another line.

Table 10. Rotational constants (MHz) for all investigated isotopes of ethyl cyanide.

		Observed[a]	Calculated[b]	Observed-Calculat.
CH_3CH_2CN	A	27 663.288 (± 0.054)	27 663.326	− 0.038
	B	4 714.199 (± 0.029)	4 713.535	0.664
	C	4 235.083 (± 0.021)	4 235.580	− 0.497
CH_3CD_2CN	A	21 942.980 (± 0.027)	21 942.983	− 0.003
	B	4 600.231 (± 0.015)	4 600.625	− 0.394
	C	4 087.830 (± 0.014)	4 087.123	0.707
CH_2DCH_2CN (sym.)	A	27 650.897 (± 0.049)	27 650.840	0.057
	B	4 425.142 (± 0.027)	4 423.749	1.393
	C	4 000.821 (± 0.019)	3 999.855	0.966
CH_2DCH_2CN (asym.)	A	25 022.652 (± 0.041)	25 022.670	− 0.018
	B	4 583.476 (± 0.022)	4 583.293	0.183
	C	4 110.264 (± 0.016)	4 110.630	− 0.366
$CH_3CH_2{}^{13}CN$	A	27 636.0[d] (± 30.0)	27 637.919	− 1.919
	B	4 689.787[c] (± 0.012)	4 689.683	0.104
	C	4 214.856[c] (± 0.012)	4 215.720	− 0.864
CD_3CHDCN	A	—	20 492.005	—
	B	4 169.499[c] (± 0.062)	4 169.477	0.022
	C	3 736.824[c] (± 0.062)	3 735.330	− 1.494

[a] Obtained from rigid rotor fits (see Tables 4, 6, 8). Except for the last two isotopes the same set of rotational lines (up to $J=2$) was used. The given uncertainties of the rotational constants are standard errors. They were used as error weights for the structure determination. As a consequence the rotational constants given for normal ethyl cyanide are slightly different from those of Table 2.

[b] Rotational constants calculated using structure in Table 9.

[c] Obtained from rigid rotor fits using the data from Reference 1. Errors are twice the standard errors.

[d] Estimated from the inertia defect of normal ethyl cyanide; $\Delta = I_c - I_b - I_a = -6.141$ amu Å^2.

Table 11. Quadrupole coupling constants (MHz).

	CH_3CD_2CN	CH_2DCH_2CN (sym.)	CH_2DCH_2CN (asym.)
χ_{aa}[a]	− 3.449 (± 0.032)[b]	− 3.326 (± 0.030)	− 3.290 (± 0.038)
χ_{bb}[a]	1.399 (± 0.030)	1.319 (± 0.028)	1.180 (± 0.036)
χ_{cc}[a]	2.050 (± 0.034)	2.007 (± 0.032)	2.110 (± 0.044)
χ_{ab}	− 2.50 (± 0.63)	− 2.61 (± 0.49)	
χ_{zz}		− 4.50 (± 0.64)	
χ_{xx}		2.47 (± 0.64)	
χ_{yy}		2.03 (± 0.06)	
η[c]		0.10 (± 0.14)	
ε		1.38° (± 0.05°)	
α_a	22.9° (± 5.1°)		
α_s[d]	19.8°		

[a] Obtained from least squares analysis including all hyperfine components from Table 3, 5, 7 up to J=2.

[b] Errors are twice the standard errors.

[c] $\eta = (\chi_{yy} - \chi_{xx})/\chi_{zz}$.

[d] Obtained from the r_0-structure of Table 9.

Quadrupole Coupling Constants

Applying the usual first order theory the diagonal elements of the quadrupole coupling tensor with respect to the principal axes of inertia for all three deuterated forms of ethyl cyanide were deduced from the hyperfine structure of the rotational lines (listed in Table 3, 5, 7). The results are given in Table 11.

For the isotopes CH_3CD_2CN and CH_2DCH_2CN (symmetric) the c principal axis of inertia coincides by symmetry reasons with a principal axis (y) for the quadrupole coupling tensor. As a consequence only one off-diagonal element (χ_{ab}) of the coupling tensor is different from zero. This value for both molecules as well as the principal elements χ_{zz}, χ_{xx} of the quadrupole coupling tensor can be obtained from the experimentally determined quantities χ_{aa}, χ_{bb} for the two molecules and from the principal axis rotation angle ε about the c-axis produced by isotopic substitution [8].

The results are given in Table 11. The comparison of the angle α_a rotating the χ-tensor to diagonal form and the angle α_s between the a-axis and the N-bond axis *, indicates a possible inclination of

* Obtained from the r_0-structure.

CN-bond direction to the z-axis of the χ-tensor. The field gradient asymmetry η points out a possible deviation from cylindrical symmetry. The uncertainties of the results which were calculated with simple Gauss error propagation law are however rather large because of the small angle ε. Within the given inaccuracies the results are in agreement with those of Li and Harmony [3] who analyzed the hyperfine structure of normal ethyl cyanide and concluded that the charge distribution about the CN-bond is cylindrically symmetric. They assumed implicitely that the CN-bond axis is colinear with the z-prinzipal axis of the quadrupole coupling tensor **.

More reliable results may be expected from the hyperfine structure analysis of the rotational lines of CD_3CH_2CN compared with CH_3CD_2CN because the angle ε will then be about twice as large as in the case considered here. This will be the object of a further investigation.

Excited Vibrational States

The two strongest sets of satellite lines which have been observed near the ground state μ_a-lines were already assigned by Laurie [2] to the rotational transitions in the first excited state of methyl torsion and the first excited state of another low frequency vibration which may be described as a "CCN-in plane" bending vibration (see below). In the following treatment these two excited states will be labelled with $v_a v_q = 10$ and $v_a v_q = 01$, respectively.

In addition to the μ_a-lines we assigned the μ_b-lines in the excited vibrational states $v_a v_q = 10{,}01$. Their assignment was difficult because of the weak absorption and the strong dependence on the A rotational constant which was only approximately given by the μ_a-transitions.

The observed rotational lines in the states $v_a v_q = 10{,}01$ – listed in Tables 12 and 13 – were fitted to Eq. (1) setting $D_k = 0$ ***. Compared with the ground state transitions the fit is rather poor. This indicates the presence of strong rotation-torsion-vibration interaction because of the near degeneracy of both vibrational states, which was already pointed out by Laurie [2] and is discussed in detail in the following sections. As a consequence of such an interaction the constants in Eq. (1), given in Table 14, can not be interpreted in the usual sense but should be regarded as empirical constants which allow a comparison of measured and calculated frequencies for assignment and a prediction of new lines.

The presense of rotation-torsion-vibration interaction in the rotational spectra is particularly indicated by the strong dependence of the effective A rotational constant on the vibrational state. The values determined for the A constant of the excited states $v_a v_q = 10(01)$ are about 2 GHz larger (smaller) than the ground state constant, whereas the B and C constants are different by only a few MHz.

In addition the excited state μ_b-lines exhibit splittings due to the internal rotation of the methyl group which cannot be interpreted by the commonly used Rigid Frame-Rigid Top (RF-RT) model theory [10, 11]. The splittings of the μ_b-type transitions in the first excited torsional state ($v_a v_q = 10$) are about 50% larger than the values obtained from RF-RT-model theory using Laurie's V_3 value [2] obtained from μ_a-line splittings. This discrepancy in the RF-RT-model cannot be removed by taking into account higher order potential coefficients for the Fourier expansion of the potential hindering internal rotation. Moreover, the μ_b-lines in the first excited CCN-in plane bend vibrational state ($v_a v_q = 01$) were also split into doublets with a mean value of approximately 1 MHz. If no interaction between this vibration and torsion takes place, these splittings should be unresolvable, as splittings of rotational lines in the ground state of both torsion and vibration have been neither expected nor observed. In order to get a more satisfactory interpretation of the measured rotational spectra we have a molecular model in which two internal degrees of freedom are considered. These are the hindered internal rotation of a methyl group about its symmetry axis and another low frequency vibration.

Hamiltonian

The quantum mechanical Hamiltonian which is used here for the analysis of the rotational spectra in the first excited states of both methyl-torsion and "CCN-in plane" bending vibration of ethyl cyanide was derived by Dreizler [12]. A more detailed treat-

** Equations (1) in Ref. 3 are only valid for $g = a, b$ if the CN-bond direction coincides with a principal axis of the field gradient tensor.

*** As only μ_b-lines with a maximal value of $K_- = 1$ were measured D_k is not determined from the experimental data.

Table 12. Rotational transitions (MHz) for the first excited torsional state ($v_a\, v_q=10$) of normal ethyl cyanide CH_3CH_2CN.

Transition $J_{K_-K_+} - J_{K_-'K_+'}$		$F - F'$	frequencies observed	unsplit	calculated[a]	$\nu_{unspl} - \nu_{calc}$
$0_{00}-1_{01}$		1 — 2	8 951.80			
		1 — 0	8 953.30	8 951.64	8 953.35	— 1.71
$0_{00}-1_{11}$		1 — 2	34 035.92			
	E	1 — 1	34 036.26			
		1 — 0	34 035.34	34 035.97		
		1 — 2	34 033.28			
	A	1 — 1	34 033.64			
		1 — 0	34 032.70	34 033.33	34 034.06	— 0.73
$1_{01}-1_{10}$		2 — 2	25 557.46			
		1 — 1	25 559.08			
	E	2 — 1	25 558.04			
		1 — 2	25 558.42			
		0 — 1	25 556.56	25 557.73		
		2 — 2	25 554.47			
	A	1 — 1	25 556.08			
		0 — 1	25 553.53	25 554.74	25 554.87	— 0.13
$1_{11}-2_{12}$				17 431.3[L]	17 432.48	— 1.18
$1_{01}-2_{02}$				17 896.9[L]	17 899.33	— 2.43
$2_{02}-2_{11}$		3 — 3	26 037.60			
	E	2 — 2	26 038.25			
		1 — 1	26 037.31	26 037.74		
		3 — 3	26 034.67			
	A	2 — 2	26 035.33			
		1 — 1	26 034.37	26 034.82	26 036.32	— 1.50
$2_{20}-3_{21}$		3 — 4	26 885.57			
	A	2 — 3	26 884.48			
		1 — 2	26 886.19	26 885.33	26 887.70	— 2.37
$2_{21}-3_{22}$		3 — 4	26 866.36			
	E	2 — 3	26 865.35			
		1 — 2	26 866.94	26 866.14		
	A	3 — 4	26 859.39			
	A	2 — 3	26 858.32	26 859.15	26 861.08	— 1.93
$2_{11}-3_{12}$				27 562.9[L]	27 565.23	— 2.33
$2_{12}-3_{13}$				26 144.2[L]	26 142.83	1.37
$2_{02}-3_{03}$				26 829.3[L]	26 830.61	— 1.31
$3_{03}-3_{12}$	E	4 — 4	26 771.12			
		3 — 3	26 771.66	26 771.29		
	A	4 — 4	26 768.25			
		3 — 3	26 768.72	26 768.39	26 770.95	— 2.56
$3_{30}-4_{31}$				35 830.4[L]	35 831.39	— 0.99
$3_{31}-4_{32}$					35 831.04	— 0.64
$3_{21}-4_{22}$	E	4 — 5	35 867.73			
		3 — 4	35 867.20	35 867.56		
	A	4 — 5	35 871.53			
		3 — 4	35 871.34	35 871.67	35 872.82	— 1.15
$3_{22}-4_{23}$	E	4 — 5	35 810.95			
		3 — 4	35 810.55	35 810.82		
	A	4 — 5	35 806.38			
		3 — 4	35 805.93	35 806.23	35 806.32	— 0.09
$3_{12}-4_{13}$	E			36 745.42		
	A			36 745.06	36 742.47	2.59
$3_{13}-4_{14}$				34 855.2[L]	34 846.20	9.00
$3_{03}-4_{04}$				35 742.5[L]	35 739.86	2.64
$4_{04}-4_{13}$	E	5 — 5	21 774.11	21 774.19		
	A	5 — 5	21 771.03	21 771.11	21 773.55	— 2.44
$4_{14}-5_{05}$	E			21 584.22		
	A			21 586.42	21 587.52	— 1.00
$5_{05}-5_{14}$	E			29 066.52		
	A			29 063.25	29 063.56	— 0.31
$5_{15}-6_{06}$	E			31 507.25		
	A			31 509.31	31 511.08	— 1.77
$6_{06}-6_{15}$	E			30 673.00		
	A			30 669.56	30 664.60	4.96

[a] Calculated with the constants from Table 14 and Equation (1).
[L] Measurements taken from Reference 2.

Table 13. Rotational transitions (MHz) for the first excited vibrational state ($v_a\, v_q = 01$) of normal ethyl cyanide CH_3CH_2CN.

Transition $J_{K-K+} - J'_{K-'K+'}$		$F - F'$	frequencies observed	unsplit	calculated[a]	$\nu_{unspl} - \nu_{calc}$
$0_{00} - 1_{01}$		1 — 2	8 964.40			
		1 — 1	8 963.35	8 964.21	8 964.38	— 0.17
$0_{00} - 1_{11}$		1 — 2	29 901.46			
	E	1 — 1	29 901.81			
		1 — 0	29 900.88	29 901.52		
	A	1 — 2	29 902.37			
		1 — 1	29 902.74	29 902.43	29 902.91	— 0.48
$1_{01} - 1_{10}$	E	2 — 2	21 407.71	21 407.98		
	A	2 — 2	21 408.66	21 408.93	21 409.05	— 0.12
$1_{10} - 2_{11}$				18 398.0[L]	18 398.55	— 0.55
$1_{11} - 2_{12}$				17 457.6[L]	17 457.52	0.08
$1_{01} - 2_{02}$				17 920.3[L]	17 920.67	— 0.37
$1_{01} - 2_{12}$		2 — 3	38 394.58			
	E	1 — 2	38 394.98			
		0 — 1	38 393.49			
		2 — 2	38 393.88	38 394.59		
	A	2 — 3	38 395.52			
		1 — 2	38 395.89	38 395.53	38 396.05	— 0.52
$2_{02} - 2_{11}$	E	3 — 3	21 885.93			
		1 — 1	21 885.63	21 886.08		
	A	3 — 3	21 886.85			
		2 — 2	21 887.55	21 887.00	21 886.93	0.07
$2_{20} - 3_{21}$		3 — 4	26 922.29			
		2 — 3	26 921.23			
		1 — 2	26 922.93	26 922.06	26 920.64	1.42
$2_{21} - 3_{22}$		3 — 4	26 889.72			
		2 — 3	26 888.67			
		1 — 2	26 890.33	26 889.49	26 889.29	0.20
$2_{11} - 3_{12}$				27 592.2[L]	27 592.28	— 0.08
$2_{12} - 3_{13}$				26 180.7[L]	26 180.81	— 0.11
$2_{02} - 3_{22}$				26 860.5[L]	26 860.82	— 0.32
$3_{03} - 3_{12}$	E	4 — 4	22 617.76			
		3 — 3	22 619.00	22 617.88		
	A	4 — 4	22 618.73			
		3 — 3	22 619.13	22 618.83	22 618.39	0.44
$3_{30} - 4_{31}$				35861.4[L]	35 862.39	— 0.99
$3_{31} - 4_{32}$					35 861.90	— 0.50
$3_{21} - 4_{22}$				35926.0[L]	35 923.45	2.55
$3_{22} - 4_{23}$				35844.6[L]	35 845.17	— 0.57
$3_{12} - 4_{13}$				36779.16	36 779.25	— 0.09
$3_{13} - 4_{14}$				34898.0[L]	34 897.67	0.33
$3_{03} - 4_{04}$				35 776.5[L]	35 776.82	— 0.32
$4_{04} - 4_{13}$	E	5 — 5	23 620.36	23 620.44		
	A	5 — 5	23 621.35	23 621.43	23 620.83	— 0.60
$4_{14} - 5_{05}$	E			25 745.32		
	A			25 744.46	25 744.67	— 0.21
$5_{05} - 5_{14}$	E			24 916.29		
	A			24 917.29	24 916.93	0.35
$5_{15} - 6_{06}$	E			35 645.03		
	A			35644.19	35 644.27	— 0.08
$6_{06} - 6_{15}$	E			26532.55		
	A			26533.58	26 534.12	— 0.54

[a] Calculated with the constants from Table 14 and Equation (1).
[L] Measurements taken from Reference 2.

ment was recently given by Mäder et alii [13]. This Hamiltonian is based on a molecular model for which the other vibrations are assumed to be negligible and for the applicability of which two assumptions are made:

(i) the internal rotor has at least C_3-symmetry about its internal rotation axis,

(ii) the configuration of the internal rotor is unaffected by the vibration.

We think that both assumptions, which lead to essential simplifications in the theoretical treatment of the model, represent a good approximation for methyl groups. Assumption (i) has already turned out to be admissible in the RF-RT-approach, al-

Table 14. Effective rotational constants [a] (MHz) for the first excited torsional and first excited vibrational state of normal ethyl cyanide CH_3CH_2CN.

	$v_\alpha v_q = 10$		$v_\alpha v_q = 01$	
A	29794.20	(±1.48) [b]	25656.24	(±0.33)
B	4713.81	(±0.38)	4717.47	(±0.09)
C	4239.66	(±0.27)	4296.95	(±0.06)
D_J	0.029	(±0.008)	0.001	(±0.002)
D_{JK}	−0.160	(±0.031)	0.120	(±0.008)

[a] Obtained from least squares analysis including all A-lines of Table 12 and 13.
[b] Standard errors.

though the r_s-structure determinations of some molecules have indicated that methyl groups are not exactly C_3-symmetric. Assumption (ii) may be justified by the fact that all normal vibrations involving methyl group deformations are rather well separated in frequency from the two low frequency vibrations considered here.

In the case of ethyl cyanide the considered vibration takes place in the symmetry plane ($y\,z$) and the Hamiltonian may then be formulated with respect to a molecule orientated coordinate system in which no angular momentum produced by the vibration exists ("Eckart-System" [13]):

$$\begin{aligned} H = {} & A(q)P_z^2 + B(q)P_y^2 + C(q)P_x^2 \\ & + D_{yz}(q)(P_y P_z + P_z P_y) - 2Q_y(q)p_\alpha P_y \\ & - 2Q_z(q)p_\alpha P_z + F(q)p_\alpha^2 \qquad (2)^* \\ & + \tfrac{1}{2}V_3(1-\cos 3\alpha) + \tfrac{1}{2}V_6(1-\cos 6\alpha) \\ & + \tfrac{1}{4}[M(q)p_q^2 + p_q^2 M(q)] + \tfrac{1}{2}k_{2q}q^2 \\ & + W(q) + \tfrac{1}{2}k_{3q}q^3 + \tfrac{1}{2}k_{4q}q^4 \\ & + V_{3c}'q(1-\cos 3\alpha) + V_{3c}''q^2(1-\cos 3\alpha) \end{aligned}$$

where

P_g operator of the total angular momentum component with respect to the g-axis of the "Eckart-System", $g = x, y, z$.

$p_\alpha = -i(\partial/\partial\alpha)$ operator of the torsional angular momentum,

$p_q = -i(\partial/\partial q)$ operator of the vibrational momentum,

q vibrational coordinate;

α torsional angle,

$$\begin{aligned} A(q) &= (h/8\pi^2)(I_{yy} - \lambda_y^2 I_\alpha)/r\Delta, \\ B(q) &= (h/8\pi^2)(I_{zz} - \lambda_z^2 I_\alpha)/r\Delta, \\ C(q) &= (h/8\pi^2)/I_{xx}, \\ D_{yz}(q) &= -(h/8\pi^2)(I_{yz} - \lambda_y\lambda_z I_\alpha)/r\Delta, \\ Q_y(q) &= (h/8\pi^2)(\lambda_y I_{zz} - \lambda_z I_{yz})/r\Delta, \\ Q_z(q) &= (h/8\pi^2)(\lambda_z I_{yy} - \lambda_y I_{yz})/r\Delta, \\ F(q) &= (h/8\pi^2)/r I_\alpha, \\ M(q) &= (h/4\pi^2)/G^{-1}, \\ r(q) &= 1 - I_\alpha(\lambda_y^2 I_{zz} - 2\lambda_y\lambda_z I_{yz} + \lambda_z^2 I_{yy})/\Delta, \\ \Delta(q) &= I_{yy}I_{zz} - I_{yz}^2, \end{aligned}$$

$I_{gg}(q)$ moments of inertia about the g-axis of the "Eckart-system" ($g = x, y, z$),

$I_{yz}(q)$ product of inertia,

λ_g direction cosine of the internal rotation axis to the g-axis ($g = y, z$),

I_α moment of inertia of the top about its symmetry axis,

$G^{-1}(q) = \sum_k m_k(\partial \boldsymbol{r}_k/\partial q)^2$ "reduced mass" for the vibration (m_k mass, and $\boldsymbol{r}_k$ position vector of atom k).

The term $W(q)$ arises from the translation of the classical to the quantum mechanical Hamiltonian. The potential energy in $H(2)$ contains a three- and sixfold term for the pure torsion (V_3, V_6), harmonic, cubic and quartic force constants for the vibration (k_{2q}, k_{3q}, k_{4q}), and two potential coupling terms, V_{3c}' and V_{3c}'', for torsion-vibration interaction. These potential coupling terms represent cubic and quartic force constants in the limit of small amplitudes of the torsional angle.

For the numerical treatment of the Hamiltonian the q-dependent coefficients of its kinetic part are expanded in power series of q up to the second order:

$$Y = Y^0 + Y'q + Y''q^2 \qquad (3)$$

with Y symbolic for A, B, C, D_{yz}, Q_y, Q_z, F, M and W. The expansion coefficients in (3) are molecular constants depending on atomic masses, molecular structure and vibrational mode. Higher order expansion coefficients are assumed to be negligible for the following analysis. The validity of this assumption will be discussed later.

Numerical Treatment

For the analysis of the spectra the energy level scheme resulting from the eigenvalues of the Hamiltonian (2) has to be compared with the experimental data. The numerical treatment of this problem is discussed in detail in Reference 13.

In order to evaluate the coefficients in (3) the r_0-structure given in Table 9 is considered to be a

* Erratum to Ref. 13: M^0 in (41 i) should be replaced by $\frac{1}{2}M^0$, $\frac{1}{2}V_{3c}''$ in (41 l) should be replaced by V_{3c}''.

good approximation for the r_0-structure, which should be known for the analysis.

The mode of the vibration considered is assumed to be approximately given by a normal coordinate analysis of the vibrational spectrum. For this purpose we utilized programs assembled by Schachtschneider et al. [14] and modified them to run on the computer systems EL X8 and PDP 10 of the University of Kiel. Using the valence force field constants given by Yamadera and Krimm [15] and comparing the results with the experimental data given by Duncan and Janz [16] and Klaboe and Grundness [17] the agreement is reasonable. The lowest frequency fundamental, which is of special interest here, was remeasured in the vapour phase using a Beckman-RIIC FS 720 Fourier interferometer and was found to have a band center at 206.5 cm^{-1} ($\pm 1.5\,cm^{-1}$) [18]. Within the normal coordinate approximation the deformation, which the molecule undergoes according to this vibration, turned out to be very sensitive to the particular choice of the force constants used. From these calculations it is evident only that this lowest frequency in-plane vibration is mainly a mixture of CCN- and CCC-angle deformation, whereby the CCC-angle increases as the N atom moves towards the *a*-axis (see Figure 1). The amount of mixing is rather undetermined by the used set of force constants. In the following treatment of the Hamiltonian the contribution of CCC- to CCN-bending is held fixed neglecting contributions of further internal coordinates. The calculations are exemplary performed for two different percentage contributions, namely 30% and 60%. We expect to get more information about the vibrational mode from the additional analysis of the vibrational spectra of other ethyl cyanide isotopes, which will be the object of a further investigation.

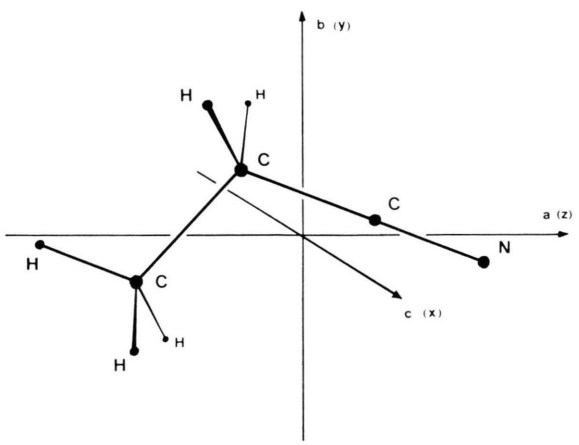

Fig. 1 Ethyl cyanide and its principal axes.

The vibrational coordinate q was chosen to be the deviation of the CCN-bond angle from equilibrium (180°) and is defined to be positive for an approach of the N atom to the *a*-axis.

With the above assumptions the components of the generalized tensor of inertia [(17) of Ref. 13] and the coefficients in the kinetic part of the Hamiltonian (2) were calculated for 11 values of q, varying q from $-5°$ to $+5°$ in steps of $1°$, and fitted to a fifth order polynomial. The expansion coefficients up to the second order for the two assumed vibrational modes are given in Table 15. The numerical method to evaluate the atomic coordinates with respect to the "Eckart-System" is somewhat different from the procedure proposed in Reference 13. Instead of Eq. (58) [13] the exact formula (53) [13] is used to calculate the angle rotating the instantaneous principal axis system to the "Eckart-System", whereby the integrand of (53) [13] is approximated by a fifth order polynomial. The partial derivatives of the coordinates with respect to q are approximated from a polynomial expansion of the cartesian coordinates, such replacing the difference quotient approximation (55) [13]. Up to second order coefficients of the fitting polynomials (Table 15) only the first and second order coefficient of G^{-1}, M and W are modified by these changes of the numerical method. Terms involving the Coriolis coupling coefficient L_x (31 i) [13], (41 g) [13] have been omitted in the Hamiltonian (2), as L_x was found to be of the order of $10^{-4}\,Hz\cdot rad$ and therefore does not influence the numerical results within the experimental uncertainties ($<50\,kHz$).

For the numerical treatment of the eigenvalue problem of the Hamiltonian (2) a system of programs was written using different sets of basis functions and employing both exact diagonalization [19] and perturbation treatment [20] of the energy matrices. This procedure allowed a mutual check of the different approaches and of the programs, as decribed in detail in Reference [13]. All results presented here are based on exact diagonalization performed for A- and E-species ** of the symmetry group of the Hamiltonian (2) [13].

** For simplification of the programs a further factorisation of the energy matrices with respect to the A_1 and A_2-species of D_3 [13] was not carried out.

Table 15. Components of the generalized tensor of inertia [a] and coefficients in the kinetic part of the Hamiltonian (2) [b].

I_{zz}°	amu Å^2	18.268 812	I_{zz}'	amu Å^2 rad^{-1}	− 13.431 923	I_{zz}'	amu Å^2 rad^{-2}	3.762 138 [c]
					− 18.087 547			4.467 407 [d]
I_{yy}°	amu Å^2	107.214 654	I_{yy}'	amu Å^2 rad^{-1}	38.885 901	I_{yy}''	amu Å^2 rad^{-2}	− 21.689 915
					56.282 352			− 26.523 640
I_{xx}°	amu Å^2	119.313 602	I_{xx}'	amu Å^2 rad^{-1}	25.453 978	I_{xx}''	amu Å^2 rad^{-2}	− 17.927 777
					38.194 805			− 22.056 233
			I_{yz}'	amu Å^2 rad^{-1}	8.404 997	I_{yz}''	amu Å^2 rad^{-2}	2.393 065
					12.618 229			0.402 620
λ_z°		0.6672	λ_z'	rad^{-1}	0.3325	λ_z''	rad^{-2}	− 0.0642
					0.479 7			− 0.1476
λ_y°		−0.7449	λ_y'	rad^{-1}	0.2979	λ_y''	rad^{-2}	0.0762
					0.4297			0.1462
$(G^{-1})^{\circ}$	amu Å^2 rad^{-2}	12.8766	$(G^{-1})'$	amu Å^2 rad^{-3}	− 5.7142	$(G^{-1})''$	amu Å^2 rad^{-4}	3.3158
		22.0776			− 12.0175			4.7269
I_{α}	amu Å^2	3.105						
A°	GHz	29.967 871	A'	GHz rad^{-1}	26.747 177	A''	GHz rad^{-2}	18.494 654
					36.319 582			38.646 224
B°	GHz	4.797 078	B'	GHz rad^{-1}	− 1.756 536	B''	GHz rad^{-2}	1.905 557
					− 2.538 808			3.118 176
C°	GHz	4.235 695	C'	GHz rad^{-1}	− 0.903 629	C''	GHz rad^{-2}	0.829 223
					− 1.355 935			1.217 072
D_{yz}°	GHz	−0.438 391	D_{yz}'	GHz rad^{-1}	− 2.654 811	D_{yz}''	GHz rad^{-2}	− 2.022 083
					− 3.936 009			− 2.670 462
Q_y°	GHz	−3.865 702	Q_y'	GHz rad^{-1}	0.820 170	Q_y''	GHz rad^{-2}	− 3.780 704
					1.115 800			− 6.317 452
Q_z°	GHz	20.321 372	Q_z'	GHz rad^{-1}	29.658 176	Q_z''	GHz rad^{-2}	19.990 883
					41.351 151			39.017 389
F°	GHz	179.19	F'	GHz rad^{-1}	24.783	F''	GHz rad^{-2}	24.661
					34.845			47.489
M°	GHz rad^2	78.495	M'	GHz rad	34.834	M''	GHz	− 4.7548
		45.782			24.920			3.7627
			W'	GHz rad^{-1}	− 13.66	W''	GHz rad^{-2}	15.51
					− 13.51			13.06

[a] see (17) of Ref. 13; [b] representation I^1 ($a \rightarrow z$, $b \rightarrow y$, $c \rightarrow x$); [c] $\measuredangle$CCN: $\measuredangle$CCC = 1 : 0.3; [d] $\measuredangle$CCN: $\measuredangle$CCC = 1 : 0.6.

Inaccuracies in the results possibly arise from the truncation of the infinite energy matrices necessary for the numerical diagonalization. By successive extension of the rank of the truncated matrices the number of basis functions which is necessary for sufficient accuracy of the results *** was estimated.

Starting with the pure torsional part of the Hamiltonian (2) which contains only torsional momentum p_{α} and torsional angle α, the corresponding energy matrix was set up in the basis of free rotor functions $-(1/\sqrt{2\pi})\exp(i\,m\,\alpha)$. For the calculation of the observed torsional states of ethyl cyanide 17 basis functions lead to sufficient precision, corresponding to a maximum value for m of 24(25) for the $A(E)$-species. The only inaccuracy arises then from rounding off errors (see below).

In the next step the energy matrix of the pure torsion-vibration part of the Hamiltonian (2), which does not contain total angular momentum components, was set up in the basis of the products of the torsional eigenfunctions $U_{v_{\alpha}\sigma}(\alpha)$ and the harmonic oscillator functions $H_{v_q}(q)$ [13]. In order to get an estimate of the number of eigenfunctions which should be taken into account for the following diagonalization of the energy matrix of the total Hamiltonian (2), we first considered the limiting cases of pure rotation-vibration and rotation-torsion (RF-RT) interaction.

The rotation-vibration interaction requires four vibrational eigenfunctions for sufficient accuracy of the rotational frequencies in the first excited vibrational state. Regarding the rotation-torsion interaction six torsional eigenfunctions are necessary for the desired precision of the rotational frequencies in the first excited torsional state.

The inclusion of torsion-vibration interaction modifies the above results. The precision of the torsion-vibration eigenvalues and of the operator

*** For the calculated rotational frequencies an accuracy better than 10 kHz was required.

matrix elements which enter into the coupling to rotation is dependent on the number of product-functions $U_{v_\alpha\sigma}(\alpha)\cdot H_{v_q}(q)$ and may be estimated from the accuracy of the rotational line frequencies by taking into account first all torsion-vibration eigenfunctions $\Phi_{v_\alpha\sigma v_q}(\alpha, q)$ [13] which result from the torsion-vibration problem and are thus available for the diagonalization of the energy matrix of the total Hamiltonian (2). Sufficient accuracy is obtained with seven torsional functions $U_{v_\alpha\sigma}(\alpha)$ and six vibrational functions $H_{v_q}(q)$ *.

In the next step it could be shown that it was possible to reduce the 42 available torsion-vibration eigenfunctions $\Phi_{v_\alpha\sigma v_q}(\alpha, q)$ in number by omitting states of high energy. The restriction to those basis function $\Phi_{v_\alpha\sigma v_q}(\alpha, q)$ which belong to the 18 lowest torsion-vibration energy states ** does not change the rotational line frequencies within the desired limits af accuracy.

Further inaccuracies in the numerical results may arise from rounding off errors. In order to get an estimate of their magnitude we compared the outcomes of X8- and PDP 10-computer runs. The double word precision of the X8-calculations with 12 decimal digits was found to be sufficient, as no change of the results within the experimental uncertainties was noted when the calculations were performed with the PDP 10 computer using double word precision with 16 decimal digits ***.

Results and Discussion

The interpretation of the measured spectra of normal ethyl cyanide on the basis of the molecular model with the two internal degrees of freedom for torsion and vibration was difficult. The time spent for the numerical calculations which were necessary for the comparison of measured and calculated frequencies was considerable *†. The dependence of the rotational frequencies on the a priori unknown potential constants in the Hamiltonian (2) is more obscure than in the RF-RT-model where in most cases only one potential constant (V_3) is determined.

In order to test the applicability of the molecular model we compared the rotational line splittings for the excited states $v_\alpha v_q = 01$ and 10 and the difference of the effective rotational constants to the ground state constants. The effective rotational constants which belong to a torsion-vibration state $v_\alpha v_q$ may be defined from the rotational transitions $J = 0 \rightarrow 1,\ 1 \rightarrow 1$ (A-species):

$$\begin{aligned} A_{v_\alpha v_q} &= \tfrac{1}{2}\left[(1_{01} - 1_{10})_{v_\alpha v_q} + (0_{00} - 1_{11})_{v_\alpha v_q}\right], \\ B_{v_\alpha v_q} &= (0_{00} - 1_{01})_{v_\alpha v_q} - C_{v_\alpha v_q}, \\ C_{v_\alpha v_q} &= (0_{00} - 1_{11})_{v_\alpha v_q} - A_{v_\alpha v_q}. \end{aligned} \tag{4}$$

For the comparison of measurement and calculation we considered only the changes of the effective rotational constants with the torsion vibration state in order to partly eliminate the influence of structural inaccuracies on the absolute line frequencies.

With (4) and the experimental data from Tables 1, 12, 13 the differences from the first to ground state constants are:

$$\begin{aligned} A_{00} - A_{01} &= 2007.55\ \text{MHz}, \\ B_{00} - B_{01} &= -3.25\ \text{MHz}, \\ C_{00} - C_{01} &= -11.69\ \text{MHz}; \\ A_{00} - A_{10} &= -2127.81\ \text{MHz}, \\ B_{00} - B_{10} &= 1.86\ \text{MHz}, \\ C_{00} - C_{10} &= -4.23\ \text{MHz}. \end{aligned} \tag{5}$$

The available experimental information was not sufficient to determine all molecular constants in the Hamiltonian (2). For that reason the constants in the kinetic part of H were held fixed as described above and an attempt was made to fit only the potential constants.

The band center frequency of the bending vibration $\omega = 206{,}5\ \text{cm}^{-1}$ ($\triangleq 6195$ GHz) – allows an approximate determination of the harmonic force constant k_{2q}. From model calculations the terms involving curvilinearity of vibrational displacements (M', M'') and kinetic vibration-torsion coupling (F', F'') as well as the terms W', W'' ** turned out to be of negligible influence ($< 0.1\ \text{cm}^{-1}$) on the vibrational frequency. With the existing infrared data the cubic and quartic force constant (k_{3q}, k_{4q}) for the vibration could not be determined.

* If the 10 kHz accuracy is only desired for the AE-splittings five vibrational functions are sufficient.

** With the published molecular constants these are the states $v_\alpha v_q$ = 00, 01, 10, 02, 20, 11, 30, 03, 21, 12, 40, 31, 04, 22, 13, 50, 41, 32 (ordered according to increasing energy).

*** PDP10 single word precision calculations (8 decimal digits) lead to frequency inaccuracies in the order of MHz.

*† For one set potential constants the evaluation of rotational frequencies up to $J=4$ takes about 55 minutes central processor unit time with PDP10 timesharing system (1 μsec cycle time).

** The additive term W^0 does not influence frequencies and has been omitted.

These constants may be deduced from 'hot band' measurements or anharmonicity constants resulting from combination bands. Model calculations with the inclusion of anharmonicity constants showed that for the evaluation of the microwave spectra only the value of the vibrational frequency is essential. These constants were therefore assumed to be zero for the following analysis. A further possible influence of the torsion-vibration potential coupling coefficients V_{3c}', V_{3c}'' on the vibrational frequency was not considered when determining the vibrational force constant k_{2q}. With the above negligences this constant is given by the vibrational fundamental frequency ω and the "inverse reduced mass" $M^0 - k_{2q} = \omega^2/M^0 -$ so that the energy level scheme resulting from the pure vibrational operator is in agreement with the infrared measurement. Possible energy level displacements by the potential coupling to torsion and the inaccurate determination of the band center frequency will be regarded in the error discussion (see below).

In order to get an estimate of the methyl-torsion barrier height, the RF-RT-model theory may be used for the analysis of the splittings of three μ_a-lines as done by Laurie [2]. It can be shown that the main contribution to these splittings arises from the diagonal matrix elements of the operator p_α in the basis of the functions $U_{v_\alpha\sigma}(\alpha)$ for E-species ($\sigma = \pm 1$). These matrix elements are assumed to be only slightly influenced by torsion-vibration interaction . Using Van-Vleck perturbation treatment [11] they lead to first order terms in the resulting effective Hamiltonian containing linear angular momentum components P_y and P_z. These linear terms are essential as the operator P_z gives rise to matrix elements connecting the rotational states $J_{K_-K_+}$ ($K_+ = J - K_-$) and $J_{K_-K_+'}$ ($K_+' = J - K_- + 1$) which are near in energy because of the small asymmetry of the molecule. Their influence to the μ_a-line splittings is sensitively dependent and maximal for rotational states with $K_- = 2$. In this case the E-species diagonal elements of p_α produce mainly the splittings. For one torsional state they do not uniquely determine one set of Fourier coefficients (V_3, V_6, ...) of the hindering potential expansion. Thus only a V_3-value of 32.8 THz (3.12 kcal/mole) * was determined from the μ_a-line splittings in the first excited torsional state ($v_\alpha v_q = 10$) with the RF-RT-model.

Taking into account a V_6-term the splittings remain the same if V_3 is suitably changed but the energy difference of ground and first excited torsional state is then modified. In default of sufficient intensity the torsional fundamental could not be observed directly in the far infrared but was deduced from combination bands of torsion and asymmetric methyl stretching or deformation vibration to be 211 cm^{-1} (see [21]). The above stated V_3-value reproducing the μ_a-line splittings implies a torsional fundamental frequency of 229 cm^{-1}. Without changing the splittings this discrepancy to the measured frequency can be removed by changing V_3 to 33.6 THz (3.20 kcal/mole) and adding a V_6-term of -2.0 THz (0.19 kcal/mole) to the Fourier expansion of the hindering potential.

These modified values for V_3 and V_6 do not yield agreement with the measured μ_b-line splittings ($v_\alpha v_q = 10$ and 01) with RF-RT-model but may be regarded as starting parameters for the following procedure which includes rotation-torsion-vibration interaction.

The Coriolis coupling operator $-2\,Q_z'\,q\,p_\alpha P_z$ which is contained in the kinetic part of the Hamiltonian (2) is the most important operator for the observed effects of rotation-torsion-vibration interaction. Its influence on the rotational line frequencies of interest here may be illustrated with a second order Van-Vleck perturbation treatment [13] aiming at the states $v_\alpha v_q = 01$ and 10. Neglecting the rotational energy differences and taking into account only the nearest torsion-vibration state, one obtains for the energy of rotational states with $K \neq 0$ second order contributions of the form:

$$\Delta H_{v_\alpha\sigma v_q} = \frac{4\,Q_z'^2\,|\langle v_\alpha\,\sigma\,v_q|\,q\,p_\alpha\,|v_\alpha \pm 1\,\sigma\,v_q \mp 1\rangle|^2}{E_{v_\alpha\sigma v_q} - E_{v_\alpha \pm 1 \sigma v_q \mp 1}} \quad (6)$$

with $|v_\alpha\,\sigma\,v_q\rangle \equiv \Phi_{v_\alpha\sigma v_q}(\alpha, q)$ torsion-vibration eigenfunctions

$\sigma = 0, \pm 1$ A,E-species of D_3.

The upper sign in (6) holds for $v_\alpha v_q = 01$, the lower for 10. The Coriolis coupling operator $-2\,Q_y'\,q\,p_\alpha P_y$, the matrix elements of which also connect the near degenerate states $v_\alpha v_q = 01$ and 10, is not considered in this rough approximation as Q_y' is small compared to Q_z' (see Table 15). Moreover the neglect of rotational energy dif-

* Because of the different structure used here, this value does not agree with Laurie's [2] work (V_3 = 32.0 THz) (3.03 kcal/mole). Instead the reduced barrier $s = 4V_3/9F^0$ is almost the same for both structures (81.3 and 81.5 resp.).

ferences is no longer valid in this case as P_y connects rotational states with different K_-. With (6) a contribution to the rotational constant A in the excited states $v_\alpha v_q = 01$ and 10 results, and its magnitude is determined by the coupling constant Q_z', the matrixelements

$$\langle v_\alpha = 0\ \sigma\ v_q = 1 \mid q\, p_\alpha \mid v_\alpha = 1\ \sigma\ v_q = 0 \rangle$$

and the energy difference of the pure torsion-vibration states. The different magnitude of the denominator in (6) for A- and E-species gives rise to different effective A-rotational constants and thus to the additional contribution to the μ_b-line splittings in the states $v_\alpha v_q = 01$ and 10.

These approximative results are confirmed by the exact numerical treatment using diagonalisation of the truncated energy matrices. The shift of the rotational constant A with torsion-vibration state and the μ_b-line splittings are sensitively dependent on the energy difference of the first excited states of torsion and vibration. The observed effects of rotation-torsion-vibration interaction should, therefore, be different for isotopic ethyl cyanides where the vibrational frequency is shifted from that of normal ethyl cyanide. The proof of this presumption will be the object of a further investigation.

In the next step of the analysis we tried to predict both the observed rotational line splittings and the differences of the effective rotational constants (5) by varying V_3 and V_6. With the assumed vibrational modes it turned out to be impossible to simultaneously fit the splittings and the line frequency shifts. This discrepancy, which could not be removed by taking into account the potential coupling coefficients V_{3c}' and V_{3c}'', may be the result of the approximations made in the molecular model and of an incorrect assumption of the vibrational mode. The influence of further vibrations which are neglected here may give rise to essential contributions to the differences of the effective B- and C-constants which are small compared to the changes of the effective A-constant with torsion-vibration state (5). A simultaneous fit of these latter changes and the rotational line splittinigs requires not only a variation of V_3 and V_6 to change the energy difference of the states $v_\alpha v_q = 01$ and 10 but also that of the parameters which determine the vibrational motion and thus part of the constants in the kinetic part of the Hamiltonian (2).

This may be seen from the estimate (6) where the vibrational mode dependence is contained in the amount of Q_z' and the matrix element of q *. Model calculations with an arbitrarily varied Coriolis coupling constant Q_z' indicate that a prediction of both line splittings and changes of the effective A rotational constant with torsion-vibration state should be possible. However it is then no longer possible to describe the vibration by a pure mixing of CCN and CCC-bending. Because of the complex way in which the vibrational motion enters into the analysis, the more elaborate treatment, which should include the variation of all vibrational mode dependent constants in the kinetic part of the Hamiltonian, was deferred.

Table 16. Potential constants of the Hamiltonian (2).

	$\measuredangle$ CCN : $\measuredangle$ CCC = 1 : 0.3	$\measuredangle$ CCN : $\measuredangle$ CCC = 1 : 0.6
V_3[a] GHz	33434 (±53)[b]	33397 (±38)
cal mole^{-1}	3176 (±5)	3173 (±4)
V_6[a] GHz	−1989 (±27)	−1942 (±19)
cal mole^{-1}	−189 (±3)	−184 (±2)
k_{2q}[c] GHz rad^{-2}	488923	838278
cal mole^{-1} rad^{-2}	46448	79636

[a] Obtained from least squares analysis including all rotational line splitting up to $J=4$. V_{3c}', V_{3c}'', k_{3q}, k_{4p} assumed to be zero.
[b] Standard errors.
[c] $k_{2q}=\omega^2/M^0$; $\omega=6195$ GHz (206.5 cm^{-1}) measured vibrational frequency, M^0 from Table 15.

In view of the reasons stated a least squares analysis for the determination of the potential constants was carried out to fit only the splittings of the rotational lines. The fitting procedure included only a variation of the Fourier coefficients V_3 and V_6 of the hindering potential. The potential coupling coefficients which may be of the order of magnitude of V_6 **, were assumed to be zero. Compared to V_3 and V_6 the influence of the potential coupling constant V_{3c}' on the energetic separation of the states $v_\alpha v_q = 01$ and 10 is very slight. Its contribution to the rotational line splittings mainly arises from the matrix element of the operator $q \cdot \cos 3\alpha$, which connects these states in the basis $U_{v_\alpha\sigma}(\alpha)$ $H_{v_q}(q)$ only for the E-species by symmetry reasons.

The split frequencies are about two orders of magnitude less sensitively dependent on V_{3c}' than

* For the uncoupled torsion-vibration basis functions $U_{v_\alpha\sigma}(\alpha) H_{v_q}(q)$ the vibrational mode dependent term in (6) is $Q_z'^2 M^0$ as $\langle v_q=0 \mid q \mid v_q=1\rangle = \sqrt{M^0/2\omega}$.
** Roughly estimated from INDO-calculations.

Table 17. Normal ethyl cyanide CH_3CH_2CN. Internal rotation splittings for the first excited torsional and vibrational state; calculated shifts of effective rotational constants and fundamental frequency for torsion and vibration.

	Transition $J_{K_-K_+} - J'_{K_-'K_+'}$	$\nu_E - \nu_A$ observed	$\nu_E - \nu_A$ calculated[b] obs.-calc. $\Delta \measuredangle CCN : \Delta \measuredangle CCC = 1 : 0.3$		$\nu_E - \nu_A$ calculated obs.-calc. $\Delta \measuredangle CCN : \Delta \measuredangle CCC = 1 : 0.6$	
$v_\alpha v_q = 10$	$0_{00} - 1_{11}$	2.64[a]	2.56	0.08	2.61	0.03
	$1_{01} - 1_{10}$	2.99	2.89	0.10	2.94	0.05
	$2_{02} - 2_{11}$	2.92	2.83	0.09	2.89	0.03
	$3_{03} - 3_{12}$	2.90	2.88	0.02	2.94	− 0.04
	$2_{21} - 3_{22}$	6.99	7.24	− 0.25	7.19	− 0.20
	$4_{04} - 4_{13}$	3.08	2.96	0.12	3.02	0.06
	$3_{21} - 4_{22}$	− 4.11	− 3.79	− 0.32	− 3.92	− 0.19
	$3_{22} - 4_{23}$	4.59	4.71	− 0.12	4.67	− 0.08
	$3_{12} - 4_{13}$	0.36	0.39	− 0.03	0.39	− 0.03
	$4_{14} - 5_{05}$	− 2.20				
	$5_{05} - 5_{14}$	3.27				
	$5_{15} - 6_{06}$	− 2.06				
	$6_{06} - 6_{15}$	3.44				
$v_\alpha v_q = 01$	$0_{00} - 1_{11}$	− 0.91	− 0.88	− 0.03	− 0.92	0.01
	$1_{01} - 1_{10}$	− 0.95	− 0.89	− 0.06	− 0.93	− 0.02
	$1_{01} - 2_{12}$	− 0.94	− 0.86	− 0.08	− 0.90	− 0.04
	$2_{02} - 2_{11}$	− 0.92	− 0.91	− 0.01	− 0.95	0.03
	$3_{03} - 3_{12}$	− 0.95	− 0.95	0.00	− 0.98	0.03
	$4_{04} - 4_{13}$	− 0.99	− 0.99	0.00	− 1.02	0.03
	$4_{14} - 5_{05}$	0.86				
	$5_{05} - 5_{14}$	− 1.00				
	$5_{15} - 6_{06}$	0.84				
	$6_{06} - 6_{15}$	− 1.03				
$A_{00} - A_{01}$[c] MHz			1264.10		1330.68	
$B_{00} - B_{01}$ MHz			− 17.56		− 16.36	
$C_{00} - C_{01}$ MHz			− 19.17		− 17.98	
$A_{00} - A_{10}$ MHz			− 1341.67		− 1450.88	
$B_{00} - B_{10}$ MHz			0.80		0.54	
$C_{00} - C_{10}$ MHz			− 7.89		− 8.22	
$\nu(v_\alpha v_q = 00 \rightarrow 10)$[d] cm^{-1}			210.1		210.5	
$\nu(v_\alpha v_q = 00 \rightarrow 01)$[e] cm^{-1}			206.3		206.5	

[a] Frequencies in MHz.
[b] Calculated with constants from Table 15 and 16.
[c] Observed values see (5).
[d] From combination bands experimentally determined to be 211 cm^{-1} (± 2 cm^{-1}).
[e] Observed value 206.5 cm^{-1} (± 1.5 cm^{-1}).

on V_3 and V_6. The inclusion of V_{3c}' in the least squares procedure yields high correlation with V_3 and V_6 and no reliable results. The influence of the potential coupling term V_{3c}'' on the line frequencies and splittings of the states $v_\alpha v_q = 01$ and 10 turned out to be negligible. From model calculations its main effect is expected to be on rotational lines of the excited states $v_\alpha v_q = 02$, 11, 20, which were not assigned.

To fit the potential constants V_3 and V_6 all line splittings up to $J = 4$ were included into the least squares procedure. Higher J-transitions could not be taken into account because of the core limitations of the available computer systems ***. The results for both assumed vibrational modes are given in Table 16 and are near the estimates obtained from the μ_a-line splittings and the torsional fundamental frequency by means of RF-RT-model theory (see above). Table 17 contains the comparison of observed and calculated splittings, the calculated shifts of the effective rotational constants with torsion-vibration state and the calculated fundamental frequencies for torsion and vibration. The variation of the amount of mixing for CCN- and CCC-bending

*** To do this, a Van Vleck transformation of second order aiming at the near degenerate pair of levels $v_\alpha v_q = (01,10)$ will be necessary. A Van Vleck transformation which aims at a single level [20] $v_\alpha v_q$ = or 01 or 10 is not sufficient in the case of ethyl cyanide.

which leads only to a slight change of V_3 and V_6 especially influences the shift of the effective A rotational constant.

This may indicate the possibility to simultaneously fit both line splittings and line frequency shifts with a modified vibrational mode which contains contributions from further internal coordinates. The torsional fundamental frequency which was obtained from combination bands (see above) and which was not included in the analysis, is predicted within the limits of the estimated error ($\pm 2\ \mathrm{cm}^{-1}$).

Regarding the possible uncertainties of the potential coefficients V_3 and V_6, the given standard errors are rather meaningless as they do not contain systematic errors which arise from inaccuracies of the molecular structure and the vibrational mode, from simplifications of the numerical treatment and from neglections made in the used molecular model.

The r_e-structure which should be known for the analysis, is approximated by a r_0-structure. The comparison with the results obtained from a preleminary structure * – $V_3 = 32371$ GHz (3075 cal/mole), $V_6 = -1326$ GHz (-126 cal/mole) [19] – indicate the influence of structural uncertainties, which are mainly due to the inaccuracy of the moment of inertia of the top I_α [22].

The influence of vibrational mode uncertainties is difficult to estimate as only two different modes were assumed in this investigation, and these modes take into account only a mixing of CCN- and CCC-angle bending. More detailed information about the molecular configuration deformation according to the considered vibration may be obtained from the vibrational analysis of isotopic ethyl cyanides.

The inaccuracy of the measured vibrational fundamental frequency is about $\pm 1.5\ \mathrm{cm}^{-1}$. This implies the same uncertainty of the energy difference of the states $v_\alpha v_q = 01$ and 10 on which the resulting μ_b-line splittings are sensitively dependent, and is therefore mainly a source of error for the potential constants V_6

$$(\Delta V_6/V_6 \cong 5\%,\ \Delta V_3/V_3 \cong 0.5\%).$$

The truncation of the fitting polynomials (3) for the constants of the kinetic part of the Hamiltonian (2) up to the second order turns out to be valid already from a classical consideration. The expansion coefficients up to the fifth order are approximately of the same order of magnitude and the mean vibrational amplitude ** for the first excited vibrational state is about 0.1 rad. As a consequence the contributions to the constants which arise from n-th order terms are about $1/10^{(n-1)}$ of the contribution from the first order term for this vibrational amplitude. These orders of magnitude, which indicate the validity of the truncation, are roughly reproduced by the results of quantum mechanical calculations up to $n = 2$. The results which were obtained by omitting the second order terms in the constants of the kinetic part of the Hamiltonian indicate that these second order terms collectively lead to contributions of about 100 KHz to the μ_b-line splittings and 200 MHz to the shifts of the effective A rotational constants. This is about 10% of the observed effects of rotation-torsion-vibration interaction which are roughly predicted by the first order terms alone. The classical estimate is thus confirmed and the neglection of third and higher order terms in (3), which are expected to change the rotational line splittings only within the experimental uncertainties, may be valid.

The potential coupling terms V_{3c}', V_{3c}'' and further potential constants which were not taken into account in the potential energy expansion of the Hamiltonian (2) could not be determined from the experimental information presently available. These constants, as well as the interaction constants to further vibrations which were not considered in the used molecular model, are contained in the given effective coefficients V_3 and V_6 of the Fourier expansion of the potential hindering the internal rotation of the methyl group.

Acknowledgements

We thank Dr. U. Andresen for many helpful discussions and for lending us computer programs. Calculations were made with the Elektrologica X8 and the Digital PDP 10 of the Rechenzentrum der Universität Kiel. We gratefully acknowledge the financial support by the Deutsche Forschungsgemeinschaft and the Fonds der Chemie.

* $r_{CH} = 1.09$ Å, $r_{CC} = 1.54$ Å, $r_{C-(CN)} = 1.47$ Å, $r_{CN} = 1.16$ Å, $\sphericalangle$ CCC = 111.01°, $\sphericalangle$ HCH = $\sphericalangle$ CCH = 109.47° (tetrahedral angle) obtained from the rotational constants of normal ethyl cyanide $CH_3CH_2{}^{13}CN$, CD_3CHDCN [19].

** Defined to be $\sqrt{|\langle v_q | q^2 | v_q \rangle|} = \sqrt{3}\, M^0/2\, \omega$ for $v_q = 1$.

[1] R. G. Lerner and B. P. Dailey, J. Chem. Phys. **26**, 678 [1956].
[2] V. W. Laurie, J. Chem. Phys. **31**, 1500 [1959].
[3] Y. S. Li and M. D. Harmony, J. Chem. Phys. **50**, 3674 [1968].
[4] H. D. Rudolph, Z. Angew. Phys. **13**, 401 [1961].
[5] U. Andresen and H. Dreizler, Z. Angew. Phys. **30**, 207 [1970].
[6] Autorenkollektiv, Organikum (8. Auflage), S. 202, VEB Deutscher Verlag der Wissenschaften, Berlin 1968.
[7] J. K. G. Watson, J. Chem. Phys. **45**, 1360 [1966]; **46**, 1935 [1967].
[8] H. Dreizler, H. D. Rudolph, and H. Schleser, Z. Naturforsch. **25 a**, 1643 [1970].
[9] H. D. Rudolph, Z. Naturforsch. **23 a**, 540 [1968].
[10] C. C. Lin and J. D. Swalen, Rev. Mod. Physics **31**, 841 [1959].
[11] H. Dreizler, Fortschr. Chem. Forsch. **10**, 59 [1968].
[12] H. Dreizler, Z. Naturforsch. **23 a**, 1077 [1968].
[13] H. Mäder, U. Andresen, and H. Dreizler, Z. Naturforsch. **28 a**, 1163 [1973].
[14] J. H. Schachtschneider and F. S. Mortimer, Vibrational Analysis of Polyatomic Molecules V, Tech. Rept. No. 231–264; Vibrational Analysis of Polyatomic Molecules VI No. 57–65, Shell Developm. Comp., Emeryville, California.
[15] R. Yamadera and S. Krimm, Spectrochim. Acta **24 A**, 1677 [1968].
[16] N. E. Duncan and G. J. Janz, J. Chem. Phys. **23**, 434 [1954].
[17] P. Klaboe and J. Grundnes, Spectrochim. Acta **24 A**, 1905 [1968].
[18] F. Winther, priv. communication.
[19] H. Mäder, Thesis, University of Kiel, Germany, 1972.
[20] U. Andresen, Thesis, University of Kiel, Germany, 1972.
[21] H. M. Heise, Diplom Thesis, University of Kiel, Germany, 1972.
[22] H. Dreizler, Conference on Critical Evaluation of Chemical and Physical Structural Information, Dartmouth College, June 24–29, 1973, Lecture 6 b.

Notiz

Singlet-Triplet Absorption Spectra of Crystalline Chrysene and Fluoranthene

L. M. Peter and G. Vaubel

Fritz-Haber-Institut der Max-Planck-Gesellschaft, Berlin-Dahlem, Germany

(Z. Naturforsch. **29 a**, 183–184 [1974]; received 16 November 1973)

The precise measurement of the absorption spectra of the spin-forbidden $S_0 - T_1$ electronic transitions in aromatic molecular crystals is usually only possible if some indirect method is used. The mutual annihilation of mobile triplet excitons in such crystals can give rise to delayed fluorescence and the excitation spectrum of this kind of emission can be related to the $S_0 - T_1$ absorption spectrum [1]. In some cases, however, the quantum yield of delayed fluorescence may not be sufficiently high to allow measurement of the excitation spectrum. Such a low yield can be due either to a low value of the triplet exciton lifetime (due e.g. to impurity quenching) or to a low value of the quantum yield of fluorescence.

An alternative method of measuring the $S_0 - T_1$ absorption spectrum involves the introduction of a suitable guest material into the crystal and subsequent measurement of the excitation spectrum of the guest phosphorescence [2]. The guest is chosen so that it effectively traps triplet excitons i.e. its triplet level must lie sufficiently below the triplet exciton band of the host crystal. At the same time the guest substance itself should have a high quantum yield of phosphorescence in the matrix isolated state. At low guest concentrations direct excitation of the guest triplet state can be neglected and indirect population takes place via the triplet exciton band of the host crystal. Consequently the observed guest phosphorescence depends linearly on the $S_0 - T_1$ absorption of the crystal (at the low intensities of excitation considered here, triplet exciton kinetics are dominated by monomolecular processes).

Pyrene (T_1 16,800 cm^{-1} [3]) was employed as the guest substance in both chrysene and fluoranthene. The polycrystalline samples containing ca. 10^{-3} mole/mole pyrene were cooled in liquid nitrogen in order to reduce the rate of thermal release of trapped triplet states into the exciton band and the red pyrene phosphorescence was measured as a function of the excitation wavelength (slit width 2 nm) in a conventional phosphoroscope arrangement. The excitation spectra obtained in this way were normalised linearly to constant excitation quantum flux density. By way of comparison the phosphorescence spectra of both chrysene and fluoranthene in methyl cyclohexane were measured and corrected for monochromator and photomultiplier characteristics.

The spectra obtained are shown in Fig. 1 and the positions of the vibrational peaks are listed in Table 1. A small red shift in the 0 – 0 transition on going from the isolated molecule to the crystal is